Polymer Journal, Vol. 38, No. 8, pp. 767–780 (2006)

The Effect of Rubber Type and Rubber Functionality on the Morphological and Mechanical Properties of Rubber-toughened Polyamide 6/Polypropylene Nanocomposites

Mat Uzir WAHIT,[1] Azman HASSAN,[1,†] Zainal Ariffin MOHD ISHAK,[2] Abdul Razak RAHMAT,[1] and Norhayani OTHMAN[1]

[1]*Faculty of Chemical and Natural Resources Engineering, Universiti Teknologi Malaysia, 81310 Skudai, Johor, Malaysia*
[2]*School of Materials and Mineral Resources Engineering, Universiti Sains Malaysia, Engineering Campus, 14300 Nibong Tebal, Penang, Malaysia*

(Received September 26, 2005; Accepted March 27, 2006; Published June 30, 2006)

ABSTRACT: Rubber toughened polyamide 6/polypropylene (PA6/PP) nanocomposites containing 4 wt % of organophilic modified montmorilonite (OMMT) were produced by melt compounding followed by injection moulding. Four different types of elastomer were incorporated into the blends as a toughener, *i.e.*, ethylene-octene elastomer (POE), ethylene-propylene elastomer (EPR), maleated POE (POEgMAH) and maleated EPR (EPRgMAH). The influences of maleating on the interfacial adhesion and mechanical properties of the nanocomposites were investigated in term of mechanical testing, the X-ray diffraction (XRD) and scanning electron microscope (SEM) observation. The results showed that modulus and strength of the nanocomposites was not significantly affected by types of elastomer and their functionality. However, the toughness of the nanocomposites toughened by maleated elastomer was higher than the unmaleated elastomer. The SEM observation revealed that rubber functionality reduces the elastomer particle size in the PA6/PP matrix due to the *in situ* formation of graft copolymer between maleated elastomer and PA6 during melt processing. XRD revealed that the type of elastomer and functionality did not affect the dispersion of the organoclay in the system. [doi:10.1295/polymj.PJ2005141]

KEY WORDS Polyamide 6/Polypropylene Blends / Rubber Functionality / Nanocomposites / Mechanical Properties / Organoclay /

Blending polyamide 6 (PA6) with polypropylene (PP) leads to materials with improved chemical and moisture resistance, dimension stability and reduced cost. However, to achieve these advantages, some form of compatibilization is generally required.[1–5] Successful approaches involved the addition of PP grafted with maleic anhydride (PPgMAH) as a third component to the blend. It is well recognized that during melt mixing process, these functionalized polymers may become *in situ* grafted with PA6 in a reaction involving succinic anhydride groups on maleic anhydride with amine end-groups of PA6, giving rise to strong links between the two phases.[1,2] However, a low notched impact strength is a common feature of these blends.[1–8] Thus considerable effort is being devoted to increase the impact toughness by adding an elastomer into the blends. For the neat PA6/PP blends, some results on incorporating of maleated POE (POEgMAH) into PA6/PP blends were published.[9,10] POEgMAH was found to be more effective than traditional modifiers such as ethylene propylene copolymer (EPR) and ethylene propylene diene copolymer (EPDM) in improving the impact strength of the blends.[9,10]

More recently, the inorganic clay minerals consisting of layered silicates were incorporated in the PA6/PP blends to form the nanocomposites.[1,2,6,7] Our previous studies showed that the PA6/PP nanocomposites are superior to the PA6/PP blends in terms of strength and modulus.[1,2] However, most of the studies on PA6/PP/organoclay reported significant decrease of toughness as compared with unfilled PA6/PP blends.[7,9] Therefore, the attempt to incorporate elastomer into the PA6/PP/organoclay becomes more desirable.

Although studies on rubber toughened polymers and rubber toughened fiber reinforced composites were extensively covered in various literatures, not much has been carried out on rubber toughened based on polymer nanocomposites system. Previous papers have shown that simultaneous use of rubber-toughening and filler reinforcement had produced a material with a balance of stiffness/strength and toughness.[11–13] It is thought that rubber toughened polymer nanocomposites may lead to a more exciting high performance material, which combines the advantages of

[†]To whom correspondence should be addressed (Fax: +607-5581463, E-mail: azmanh@fkkksa.utm.my).

Table I. Polymer materials and clay used in this study

Material (designation used here)	Commercial Name	Description	Source
Polyamide 6 (PA)	Amilan CM1017	MFI (g/10 min, 190 °C/2.16 kg,) − 25	Toray Nylon Resin, Japan
Polypropylene (PP)	SM 240	MFI (g/10 min, 190 °C/2.16 kg,) − 25	Titan Polymer, Malaysia
Polypropylene grafted maleic anhydride (PPgMAH)	Orevac CA 100	MAH graft level − 1% MFI (g/10 min, 190 °C/325 g) − 10	Atofina, France
Ethylene octane elastomer (POE)	Engage 8150	Comonomer content, wt % - 39 MFI (g/10 min, 190 °C/2.16 kg, dg/min) − 0.5	Dupont Dow Elastomer, USA
Ethylene octane elastomer grafted maleic anhydride (POEgMAH)	Fusabond N MN493D	Density − 0.87, Medium MAH graft level, MFI (g/10 min, 190 °C/2.16 kg) − 1.6	Dupont
Ethylene propylene elastomer (EPR)	Vistalon 878	Ethylene content wt % - 59.7	Exxon Mobil
Ethylene propylene elastomer grafted maleic anhydride (EPRgMAH)	Exxelor VA 1801	Semi-crystalline MFI (g/10 min, 230 °C/10 kg) − 9 Tg - -57 °C	Exxon Mobil
Organoclay	Nanomer 1-30TC	Montmorillonite intercalated by octadecylamine	Nanocor, USA

rubber-toughening and the merits of polymer nanocomposites. This is based upon earlier studies on layered silicates polymers nanocomposites which have generated interesting results of strength and stiffness enhancement at low filler concentrations.

In a recent study, we described the preparation of POE toughened PA6/PP nanocomposites by direct melt compounding, *i.e.*, simultaneous addition of all components to a co-rotating twin-screw extruder.[14,15] However, it has limited success due to insufficient compatibility between PA6 and POE. In order to improve the compatibility between PA6 and the POE phase, POEgMAH was used in the current research. So far, no study has been reported on the use of POEgMAH as toughening agent for PA6/PP nanocomposites. The incorporation of POEgMAH to PA6/PP nanocomposites is expected to have an important effect on the morphology and mechanical properties of these materials, and this issue is examined here. Beside that, traditional modifiers; ethylene propylene rubber (EPR) and maleated ethylene propylene rubber (EPRgMAH) were also used for comparison purpose. The maleic anhydride group grafted to the rubber is expected to react with amine end groups of the PA6 forming a graft copolymer that helps to disperse the rubber particles. The structural and mechanical properties of the formed nanocomposites and the effect rubber functionality will be investigated using X-ray diffraction (XRD), Scanning Electron Microscope (SEM) and mechanical analysis.

Table II. Materials designation and compositions

Designation	Composition (wt %)			
	PA6/PP (70:30)*	PPgMAH	Organoclay	Elastomer
BC	95	5		
BCF	91	5	4	
BCF/POE	81	5	4	10
BCF/mPOE	81	5	4	10
BCF/EPR	81	5	4	10
BCF/mEPR	81	5	4	10

*The ratio of the mass.

EXPERIMENTAL

Materials and Sample Preparation

Tables I and II show the materials and formulations used in this study, respectively. Nanomer 1.30 TC is surface modified montmorillonite minerals. They are designed specifically for extrusion compounding. Four commercial grades of elastomer and maleated elastomers referred here as POE, EPR, POEgMAH, and EPRgMAH were used to form rubber-toughened PA6/PP nanocomposites. Prior to each processing step, all PA6 containing material was dried at 80 °C for at least 16 h to avoid moisture induced degradation reactions. The extruded pellets were injection moulded into standard tensile, flexural and Izod impact specimens using a JSW Model NIOOB II injection-moulding machine with the barrel temperature of 210–240 °C. Specimens were tested dry as moulded.

X-Ray Diffraction

X-Ray diffraction (XRD) measurements were made directly from montmorillonite and organoclay powders. In the case of nanocomposites blends, measurements were carried out on tensile bar cut. All these experiments were performed using Siemens XRD. The XRD spectra of samples taken from injection-moulded specimens (normal to flow direction) of the nanocomposites. The XRD were recorded with a step size of 0.02° from $2\theta = 1.5$ to 10°. The interlayer spacing of organoclay was derived from the peak position (d_{001}-reflection) in XRD diffractograms according to Bragg equation.

Microscopy Examination (SEM)

The morphology of the blends was examined using a Philips scanning electron microscope. Samples were cryogenically fractured in liquid nitrogen and etched in heptane at 50 °C for 3 h to extract the elastomeric POE phase. Samples were coated with gold prior to examination under the electron beam. An operating voltage of 10 kV was used. The size distribution of POE phase in blends was determined by measurement of approximately 200 domains from sets of cryo-fractured micrograph using Zeiss KS 300 Imaging System Release 3.0 software.

Mechanical Testing

Tensile and flexural tests were carried according to ASTM 638 and ASTM 790 methods, respectively using an Instron 5567 Universal Testing Machine under ambient condition. The crosshead speeds were 50 mm/min and 3 mm/min, respectively. The Izod impact tests were carried out on notched specimens using Toyoseiki impact tester at ambient conditions. In all cases, five specimens of each were tested and the average values were reported.

RESULT AND DISCUSSION

Mechanical Properties

The Effect of Incorporation of Organoclay and Elastomer. Typical stress-strain curves for the blends and nanocomposites are given in Figure 1. For the pristine PA6/PP blends, the samples displayed the typical characteristics of a ductile thermoplastic, *i.e.*, stress whitening followed by necking and drawing. However, the incorporation of the organoclay into the blends reveal the fragile room temperature behaviour of the PA6/PP/organoclay as compared to the reference PA6/PP blends with a strain at break as little as 4–5%. The elongation at break slightly increases with the incorporation of rubber indicating that the nanocomposites become more ductile. However, a fairly large ductility was only observed for the nanocomposites incorporated with the maleated rubber.

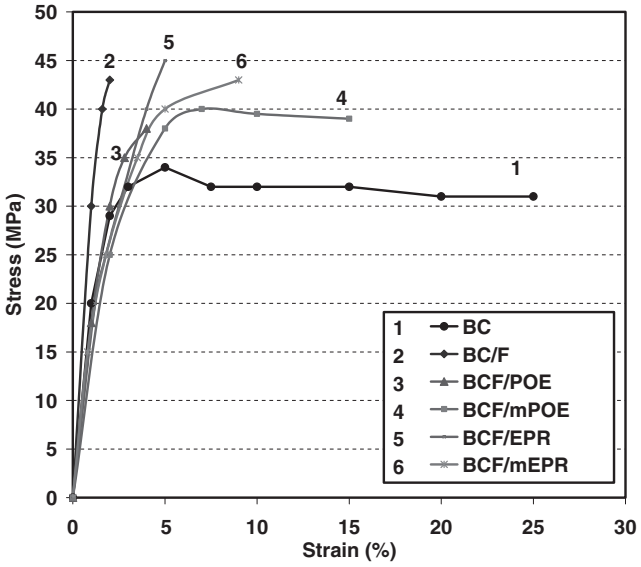

Figure 1. Stress-strain curve for various rubber toughened PA6/PP nanocomposites.

The strength, stiffness and toughness of the neat PA6/PP, PA6/PP/organoclay and PA6/PP/POE blend are shown in Figures 2–4. As can be seen in Figures 2 and 3, the incorporation of the organoclay in the presence of compatibilizer has led to the enhancement of both strength and stiffness of the nanocomposites. Similar improvements in mechanical properties were also reported by previous researchers.[16–20] According to Liu *et al.*,[19] generally the reinforcing effect of the organoclay on the stiffness and the strength was due to the incorporation of clay platelets into polymer matrix which is higher in the modulus than the polymer. The organoclay are able to act as reinforcing filler for the polymer matrix due to its high aspect ratio and platelet structure. In addition, the stiffness of the silicate layers contributes to the presence of immobilized or partially immobilized polymer phase.[19]

Beside that, the incorporation of PPgMAH causes the formation of the polyamide 6 grafted polypropylene (PA6gPP) copolymer which strengthened the interface between the PA6 and PP phases (see Figure 5). The reaction of the graft copolymer formation was previously proposed by Duvall and co-workers[21] and has been confirmed through solvent extraction. The grafted copolymers preferentially reside at the interface and improve interfacial adhesion through the chemical linkage across the interfaces.[21,22] Besides, there was a strong interaction between the PA6 matrix and the silicate layers. It is believe that the hydrogen bonding could form between the amide group of the PA6gPP copolymer and octadecylamine group of the organoclay intercalant (see Figure 5). According to Chow *et al.*[1,2] this amide-amine reaction could happen

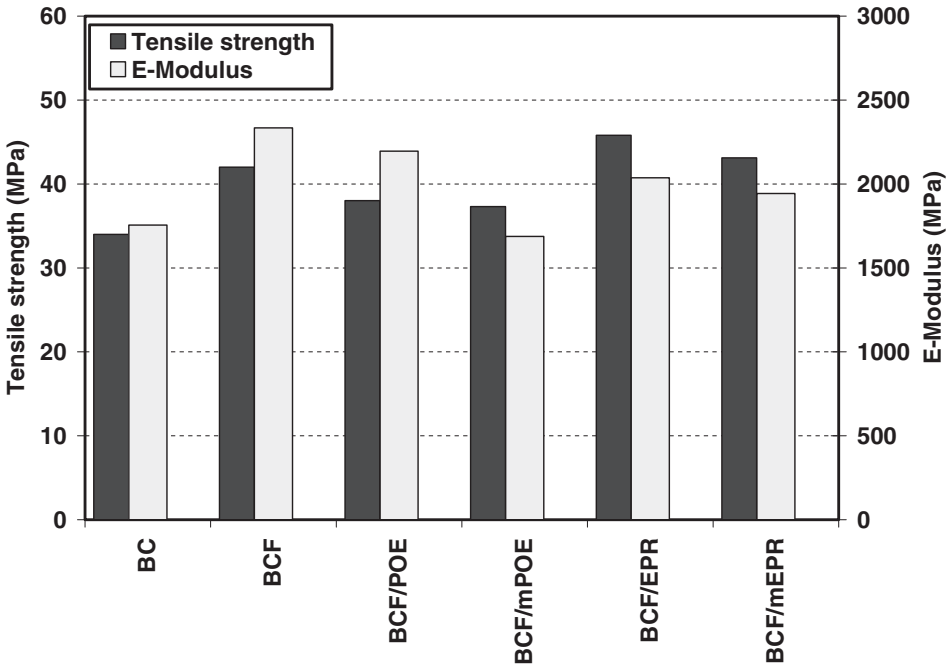

Figure 2. Tensile strength and E-modulus of rubber toughened PA6/PP nanocomposites with different type of elastomer.

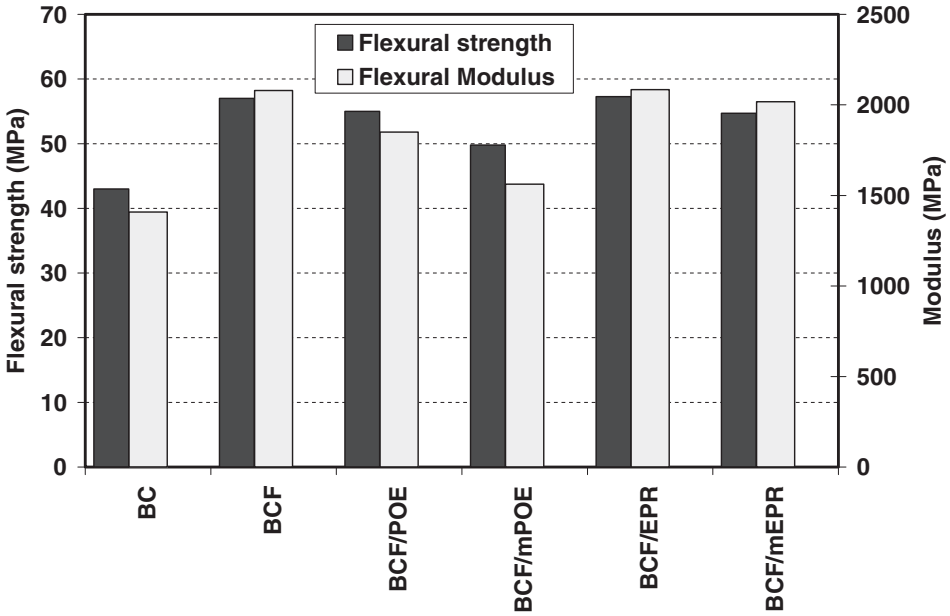

Figure 3. Flexural strength and flexural modulus of rubber toughened PA6/PP nanocomposites with different type of elastomer.

when the organoclay was exfoliated in the PA6/PP matrix, subsequently the octadecylamine (intercalant) is capable to form a chemical linkage with PA6gPP copolymer.

The effect of incorporating organoclay on the elongation at break and impact strength of the blends is illustrated in Figure 4. The presence of organoclay appears to override the toughening effect of the PA6/PP blend. This observation is generally found in nanocomposites system. A similar result was obtained by Wang and co-workers[6] where the addition of 5 wt % organoclay in PA6/PP/PP-g-MA blends shows lower impact strength as compared to the neat blends. According to Stevenson,[23] there are two main reasons why filler have detrimental effects on the impact performance. One important reason is that a significant volume fraction of the polymer, which can dissipate stress through the shear yielding or crazing mechanism, is replaced by the filler, which is generally cannot deform and dissipate the stress easily. The total ability of the material to dissipate the stress is therefore decreased. However, this is particularly true at

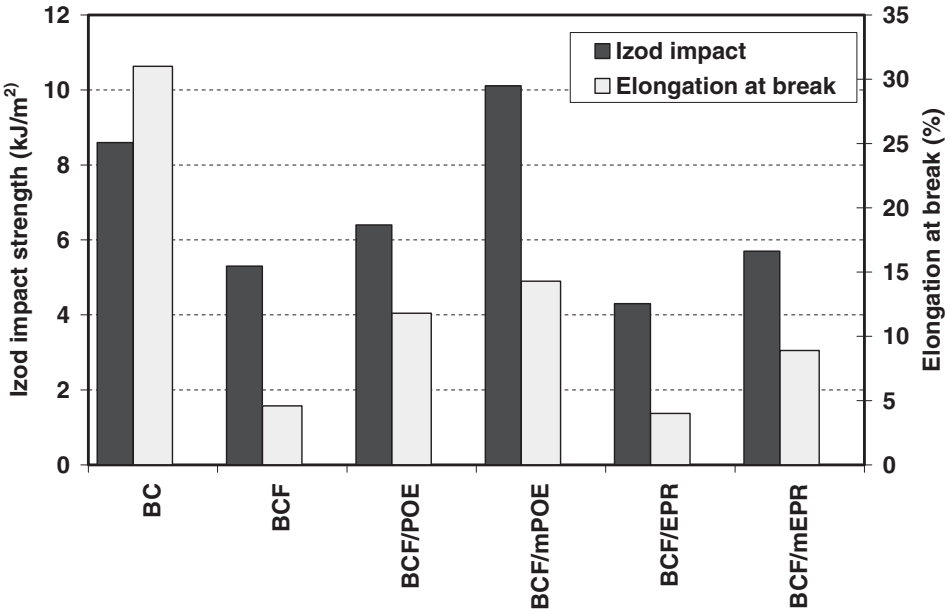

Figure 4. Izod impact strength and elongation at break of rubber toughened PA6/PP nanocomposites with different type of elastomer.

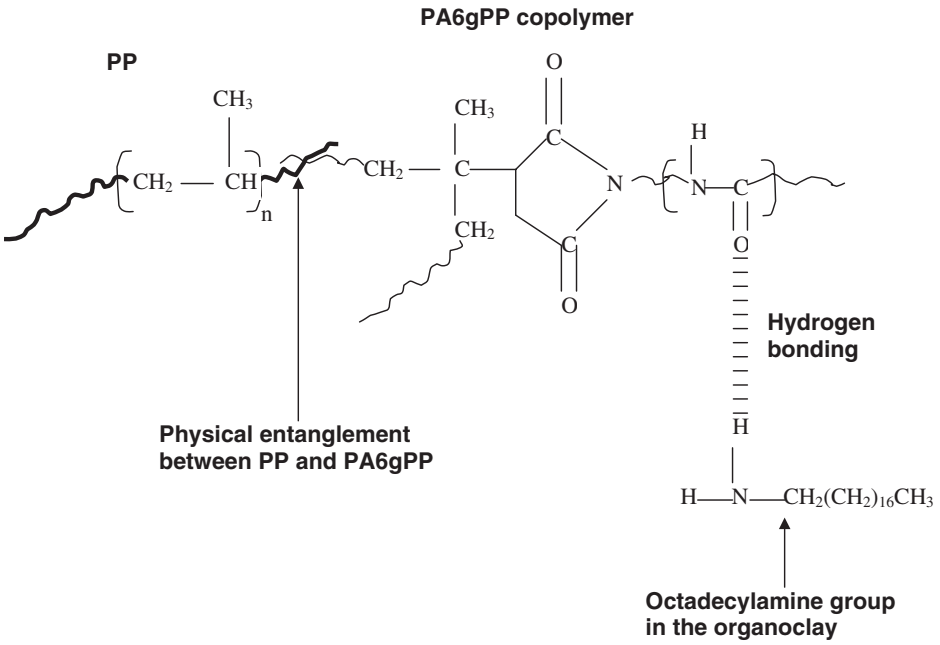

Figure 5. Interaction between PA6gPP copolymer, PP and organoclay.

high concentration of filler. It is also possible that either polymer nanocomposites inherently contain incomplete dispersion of nanoparticles, which form aggregates, that cause premature crack formation, or the presence of exfoliated nanoparticles restricts molecular mobility of the surrounding matrix material, which leads to embrittlement or both.[24]

The result presented in Figures 2 and 3 show that in general, simultaneous use of rubber toughening (for all types of rubber) and organoclay (PA6/PP/organoclay/elastomer) cause a reduction in the stiffness and strength of the blends as compared to the PA6/PP/organoclay blends. This observation is generally found in various blends and has been reported to be due to the softening or diluting effect of the second component.[25,26]

Figure 4 shows the toughness properties as indicated by the impact strength and elongation at break of the blends with different type of elastomer. It is obvious that the impact strength of the PA6/PP/organoclay increase with the incorporation of elastomer. Even though the incorporation of unmaleated elastomers did increase the toughness of the PA6/PP/organoclay, the impact strength values are still lower than

that of neat PA6/PP. Contrarily, better improvement in toughness properties was achieved in the blends incorporated with the maleated rubbers. This will be discussed in more details in next section.

The Effect of Types of Elastomer

The effect of different types of elastomer on the mechanical properties of PA6/PP blends and its nanocomposites are shown in Figures 2–4. The rubber-toughened nanocomposites using EPR and maleated EPR displayed a slightly higher tensile strength and E-modulus compared to the nanocomposites containing POE and maleated POE. Similar trend was observed in flexural properties. According to Laura *et al.*,[11] the characteristics of the leastomer are important to blend performances. The higher tensile strength and modulus of EPR elastomer as compared to POE probably accounts for the higher values for tensile strength and modulus of the nanocomposites containing EPR. Laura and co-workers[11] found the same trend in PA6/SEBS/glass fibers and PA6/EPR/glass fibers. The SEBS elastomer which has a higher tensile strength and modulus than EPR caused higher strength and stiffness in the PA6/SEBS/glass fibers system as compared to PA6/EPR/glass fibers system.

Interestingly, the impact properties and elongation at break of both POE and POEgMAH PA6/PP/organoclay are higher than the corresponding EPR nanocomposites (Figure 4). This could be attributed to the differences in rubber structure, the The smaller particle size of POE and POEgMAH over that of EPR and EPRgMAH may be responsible for such observation. This was due to similarity in chemical composition between PP and POE which subsequently helps the interaction between them. In addition, the presence of ethylene phase in PP copolymer in our study may further improve compatibility between PP and POE. Even though PP and EPR are not miscible, there is limited affinity that leads to good adhesion between the phases.[1,2]

The Effect of Rubber Functionality

Figures 2 and 3 depict that the nanocomposites toughened with maleated rubber show lower tensile and flexural properties than the nanocomposites with unmaleated rubber. This finding seems to be consistent to previous works reported by Yu *et al.*[26] and Premphet-Sirisinha and Chalearmthitipa.[27] They attributed the lower modulus of PA6/maleated POE as compared to the PA6/POE blends was due to the changes of morphology of the PA6 caused by graft modification of POE. Cimmino *et al.*[28] reported a similar observation in their work on the mechanical properties of the PA6/maleated EPR and the PA6/unmaleated EPR. The reason was reported to be the graft copolymer (EPRgMAH)gPA6 at the interfacial zones between PA6 and the dispersed particles, which caused an increase in free volume. The higher free volume, the more room the molecules will have in which to move around and the lower will the glass transition temperature (T_g).

The contrasting effect can be seen for impact strength and elongation at break values (see Figure 4). The nanocomposites containing maleated rubber exhibited higher impact strength and elongation at break as compared to unmaleated rubber. This indicates that addition of non-reactive rubber has mildly contributed to the improvement of notched impact strength of the nanocomposites. Even though the incorporation of non-maleated elastomer did increase the toughness of the nanocomposites, they are not able to fully compensate for embrittlement caused by the presence of organoclay. In addition, the inferior properties may also be attributed to high polarity differences between non-maleated elastomer and PA6, making this binary blend as immiscible system. This leads to nanocomposites with poor impact properties.

It can be seen that the nanocomposites toughened by POEgMAH posses the highest toughness values with impact strength two times higher than PA6/PP/oganoclay and elongation at break of 14.3%. This provides a good indication of the effectiveness of POEgMAH as toughening agent for PA6/PP/organoclay nanocomposites. The increase in impact strength and elongation at break suggests better stress transfer across the interfaces in the nanocomposites and blend containing maleated rubber.[27] According to Yu *et al.*,[26] if the rubber phase is highly dispersed, it can acts as an effective stress concentrator and enhances both crazing and shear yielding in the matrix. Both processes are capable of dissipating larger amount of energy which will then leads to a significant increase in the toughness of the blends.

The Effect of POE and Maleated POE Concentration

The effects of both ummaleated and maleated POE on tensile and flexural strength are illustrated in Figures 6 and 7. It can be seen that both tensile and flexural strength decreases steadily with increasing POE content. Irrespective of rubber content, there is no significant difference in tensile and flexural properties between the nanocomposites toughened with either POE or maleated POE.

However, a more interesting trend can be observed for the impact strength. Figure 8 shows the impact strength as a function of elastomer concentration for both types of POE. It is can be seen that the impact strength of the nanocomposites increases with the elastomer content. The improvement was not that sig-

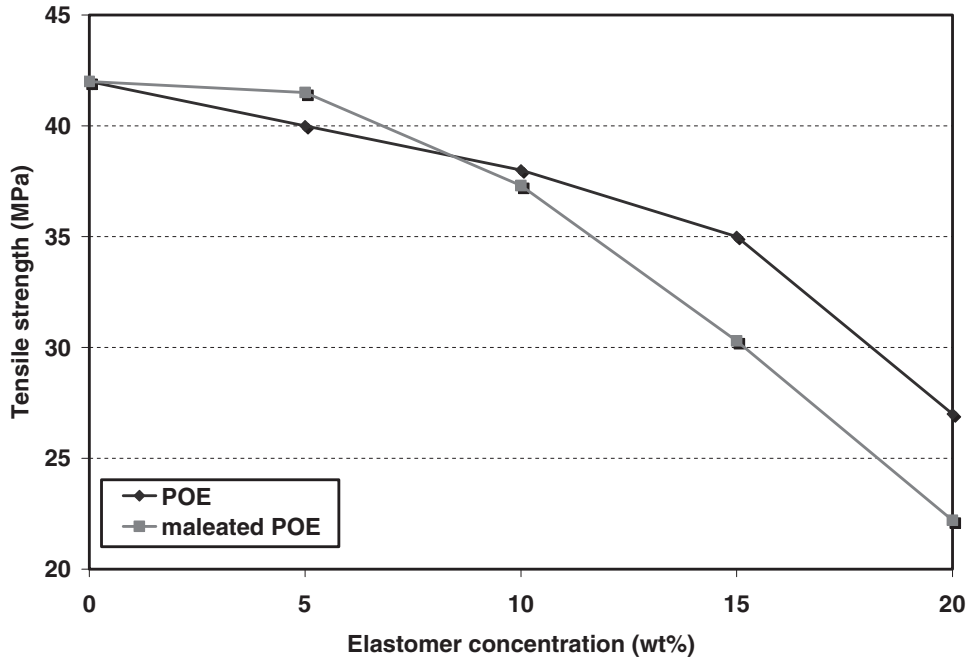

Figure 6. The effect of elastomer content on the tensile strength of rubber toughened PA6/PP nanocomposites.

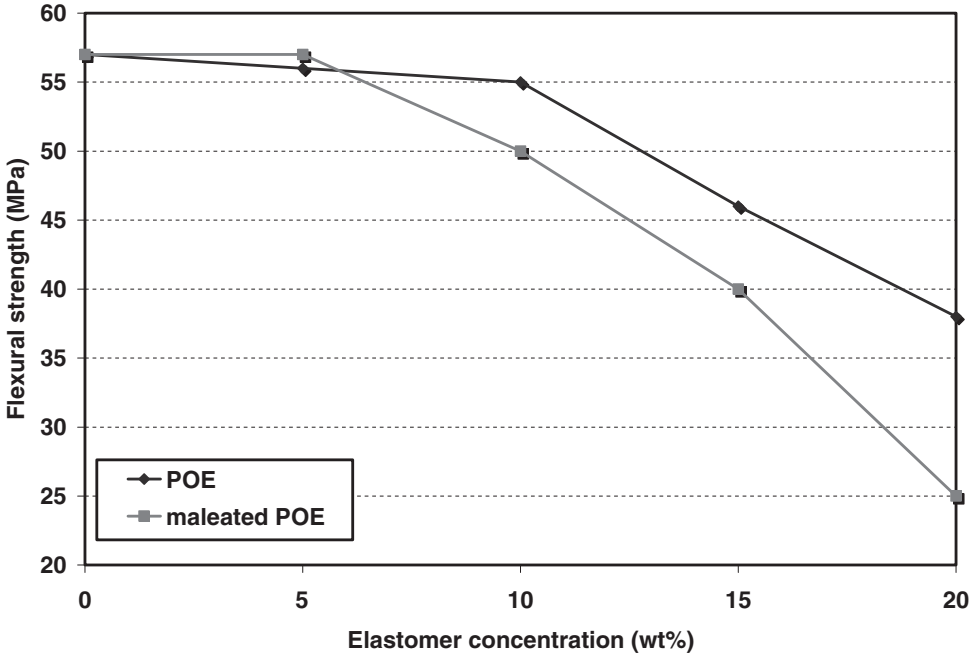

Figure 7. The effect of elastomer content on the flexural strength of rubber toughened PA6/PP nanocomposites.

nificant for the POE system. However, a remarkable improvement in the impact strength was observed for the nanocomposites filled with maleated POE. An impact strength of 37 kJ/m^2, *i.e.*, four times higher than that PA6/PP blends was recorded for POEgMAH system. Yu *et al.*[26] obtained around five times improvement in the notched impact strength of the PA6 with the incorporation of 20 wt % of maleated POE. The functional group in POE is believed to react with terminal groups of PA6 thus improving the distribution of POE elastomer particles in the PA6/PP matrix. This is well supported by the qualitative evidences obtained from SEM examination as will be reported later.

X-Ray Diffraction

In Figure 9, the XRD paterns of rubber toughened PA6/PP nanocomposites with different types of elastomer are shown along with those of the pristine organoclay 1.30TC. As expected, the organoclay 1.30TC

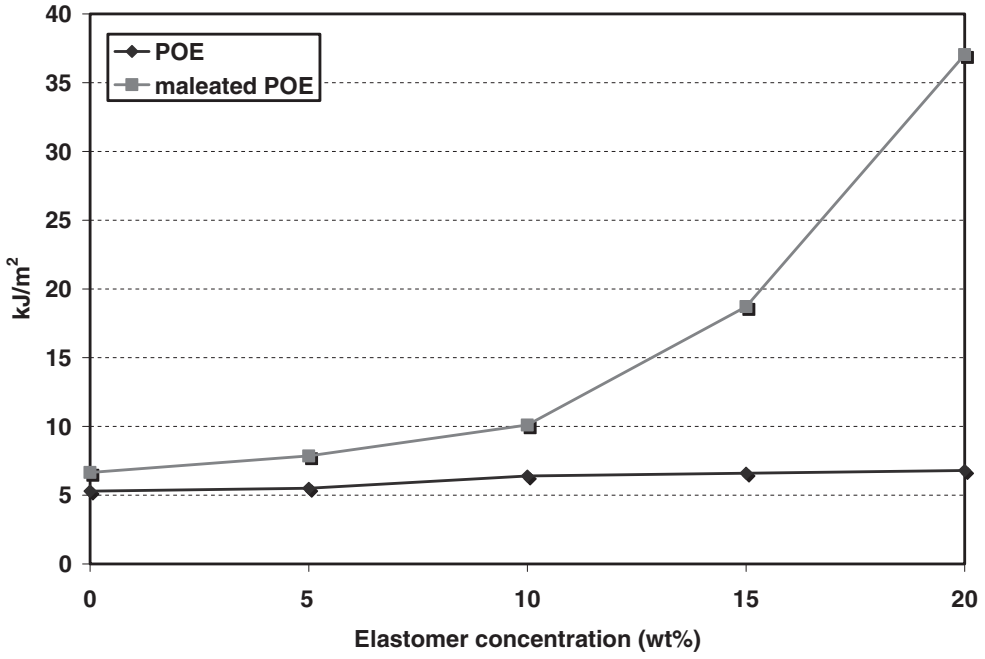

Figure 8. The effect of elastomer content on the impact strength of rubber toughened PA6/PP nanocomposites.

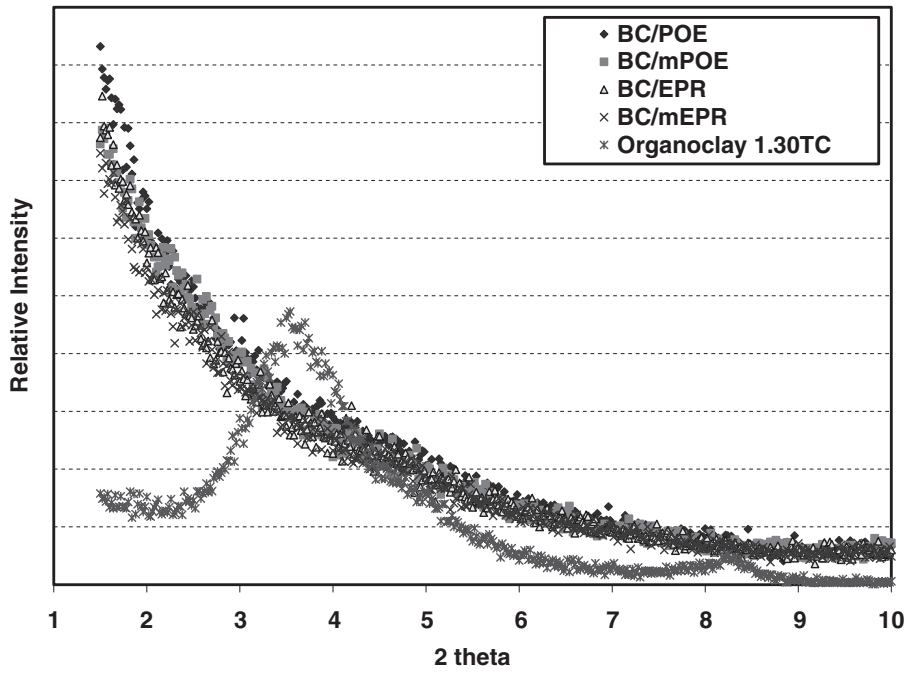

Figure 9. XRD spectra for the organoclay and PA6/PP nanocomposites with different type of elastomer.

spectrum shows a peak centered at about $2\theta = 3.5^\circ$ corresponding to a d-spacing of 2.49 nm. After incorporating the organoclay into elastomer modified PA6/PP blend, the basal plane of organoclay disappears regardless of the types of elastomer added. The absence of basal plane peaks is a strong evidence for the formation of an exfoliated nanocomposites structure.[7,18] The study also revealed that, the usage of different types of elastomer does not change the distribution of the clay in the matrix.

Morphology

Figures 10(a) and 10(b) presents the cryo-fractured surfaces by heptane of the PA6/PP blends nanocomposites toughened with POE and POEgMAH, respectively. The black pits correspond to sites where elastomer particles were extracted from PA6/PP matrix. The SEM micrograph in Figure 10(a) presents the homogenous character of the morphology of the blends. However, the immiscibility between POE and PA6 resulted in phase separation of POE particles

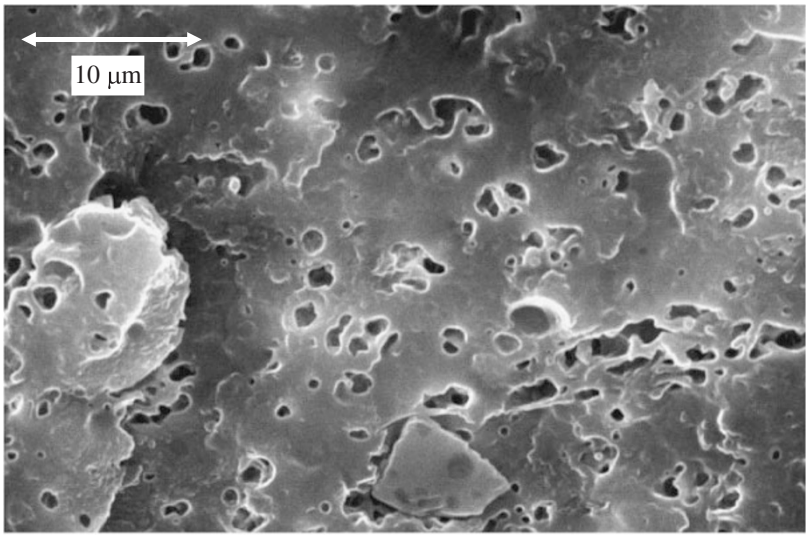

(a)

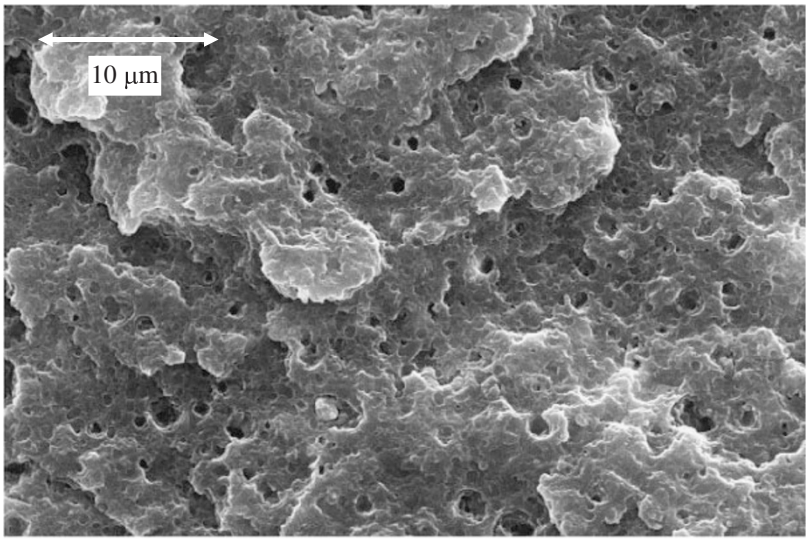

(b)

Figure 10. SEM micrographs of cryo-fractured surfaces by heptane of PA6/PP/organoclay toughened by (a) POE, (b) maleated POE.

in the blends. The edges of the holes where POE have been extracted are quite smooth. This confirms that a weak interfacial adhesion between the two phases which arises as a result of the poor compatibility between PA6 and POE. A similar result was observed for the nanocomposites system toughened with EPR and EPRgMAH as shown in Figure 11.

In order to have an efficient stress transfer between two phases, the rubber particles should be well dispersed so that they can act efficiently as stress concentrator, and they should be well bonded to polymer matrix.[29] In this work, when PA6/PP/elastomer blend cooled from the melt, most elastomer will shrink more than the polymer matrix. For the PA6/PP/unmaleated POE blend, the debonding will thus occur because the absence of good adhesion between POE and PA6/PP phase.

As mentioned earlier the succinic anhydride group of the maleic anhydride grafted POE is able to react with PA6 terminal group to form POEgPA6 copolymer that strongly tends to concentrate at PA6/PP interfaces during melt processing.[10] According to Liang and Li,[30] when rubber was grafted with suitable content of MA, the rubber particles were dispersed uniformly in the continuous PA6 matrix and the PP was encapsulated by thin layers of rubber (*i.e.*, shell-core structure). When highly dispersed, the rubbery phase act as an effective stress concentrator and enhances both crazing and shear yielding in the matrix. Since both processes can dissipate large amount of energy, there is significant increase in the toughness of the nanocomposites toughened with POEgMAH.[26]

Table III summarized the size distribution of POE domain from measurement of a set of SEM micro-

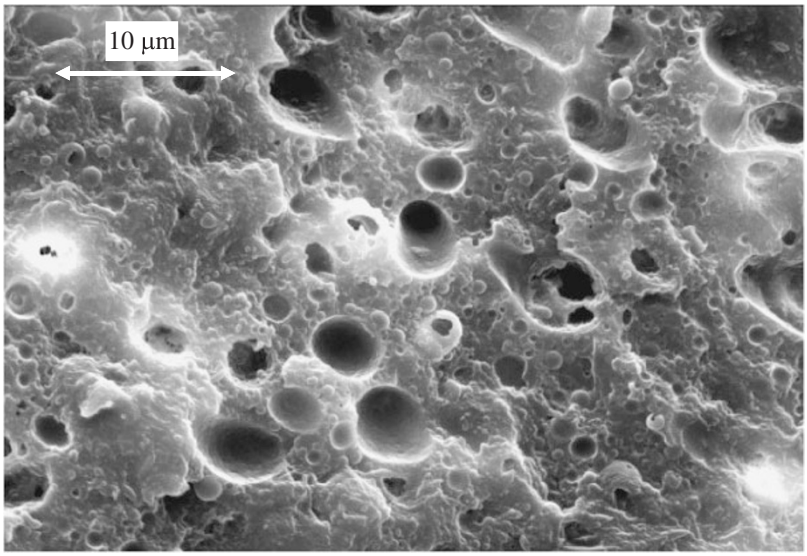

(a)

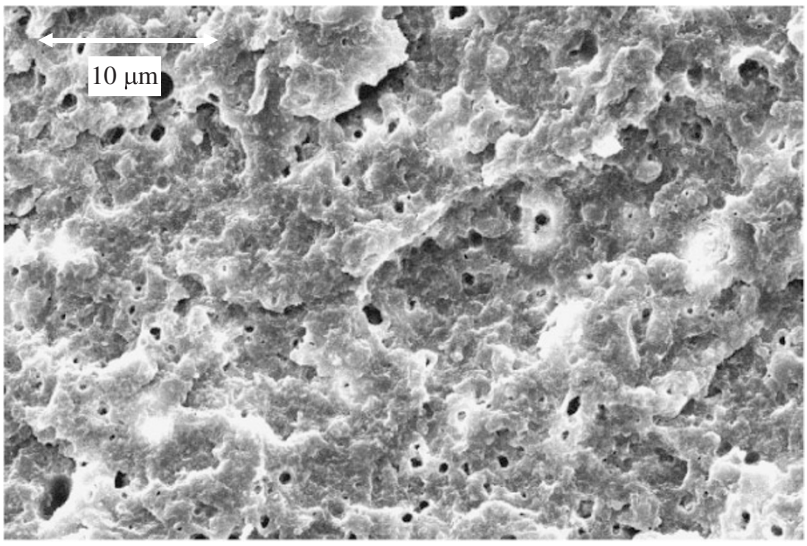

(b)

Figure 11. SEM micrographs of cryo-fractured surfaces by heptane of PA6/PP/organoclay toughened by (a) EPR, (b) maleated EPR.

Table III. The average of elastomer particle size in PA6/PP nanocomposites

Blend/Elastomer	Diameter Range (μm)	Average Particle Diameter (μm)
BCF/POE	0.66–2.54	1.50
BCF/mPOE	0.50–2.80	0.96
BCF/EPR	0.18–3.95	1.39
BCF/mEPR	0.10–1.90	0.81

graph on cryo-fractured surfaces. The nanocomposites containing POEgMAH shows morphology of fine particle with an average diameter of 0.96 μm, which is relatively smaller than those observed in the nanocomposites blend of unmaleated POE (1.50 μm) of the same composition. Besides that, the maleated POE particles are also more uniformly distributed as shown by the SEM micrograph in Figure 10. This seems to suggest the reduction of the interfacial tension of the blend in the presence of POEgMAH has not only reduces the particles sizes of POE but also improved the dispersion of POE in the PA6/PP matrix. Similar finding have been reported for PA6/POEgMAH blends.[27] The enthalpy of the system that drove the POEgMAH-g-PA6 to the interface was reported to cause an increase in the interfacial area and a reduction in rubber particles size. Thomas and Groenicky[31] also observed that the addition of maleated EPR reduced the domain size of EPR dispersed phase in the PA6 blends.

The SEM micrographs of the fracture surfaces resulting from the impact test for the nanocomposites toughened with 20 wt % of POE (BCF/POE) and maleated POE (BCF/mPOE) are shown in Figure 12.

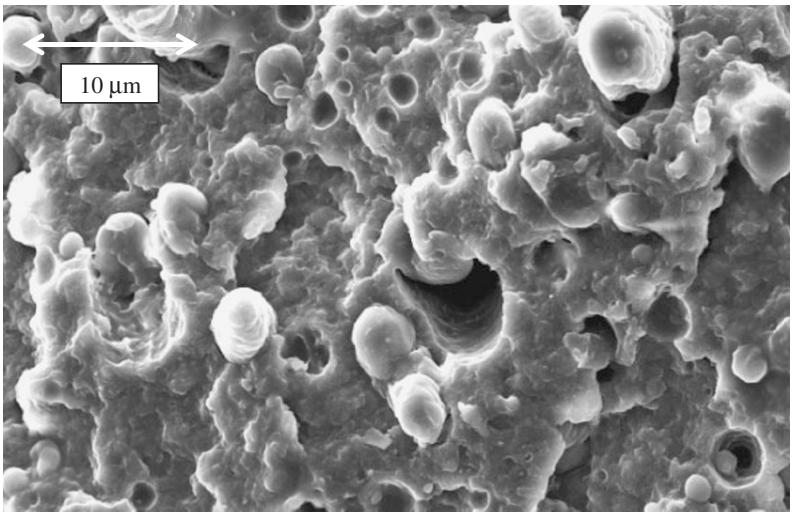

(a)

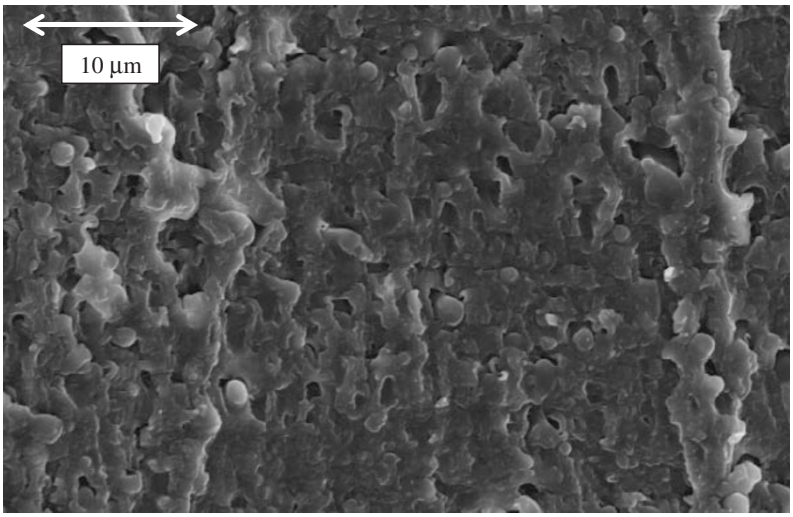

(b)

Figure 12. SEM micrographs of impact fracture surfaces of the PA6/PP/organoclay with 20 wt % elastomer content (a) POE, (b) POEgMAH.

Noted that the impact strength of the BCF/POE and BCF/mPOE are 6.8 and 37 kJ/m^2, respectively. It is evident that the morphologies of the fracture surfaces for the two blends are quite different. In the case of the nanocomposites containing POE, large holes are clearly observed, formed by the removing of the POE particles. Moreover, it can be seen that the fracture surface is smooth, indicating that the matrix PA6/PP fractures in a brittle manner during impact. In the case nanocomposites containing maleated POE, holes are slightly elongated or distorted and the outline of the holes is indistinct. The higher value of elongation at break and impact strength obtained for the BCF/mPOE may arise as a consequence this elongated phase morphology of the maleated POE in the PA6/PP matrix. The significant difference in impact strength between BCF/POE and BCF/mPOE can be ascribed to the fact that the former nanocomposites fractures in brittle mode, whereas the latter one fractures in ductile mode.

Interpretation of SEM micrograph showing on how the POE and POEgMAH affects the morphology of PA6/PP blends and their impact properties will be aided by the schematic shown in Figures 13 and 14. This interpretation was based on the SEM micrograph and some related work on PA6/PP/SEBS and PA6/PP/SEBSgMAH blends.[3–5] Binary blends of different components of rubber-toughened blends have similar morphologies; dispersed phase of one component in a matrix of remaining component. However, the rubber domains in the PA6/maleated POE blends are smaller than the rubber domains in PA6/POE due to the reaction that take place between PA6 and maleated POE during melt processing.[14,15] In the ternary blends of PA6/PP/PPgMAH/POE, some of the rubber tends to locate in the PP and at the interface between PA6 and PP and the remainder tends to be dis-

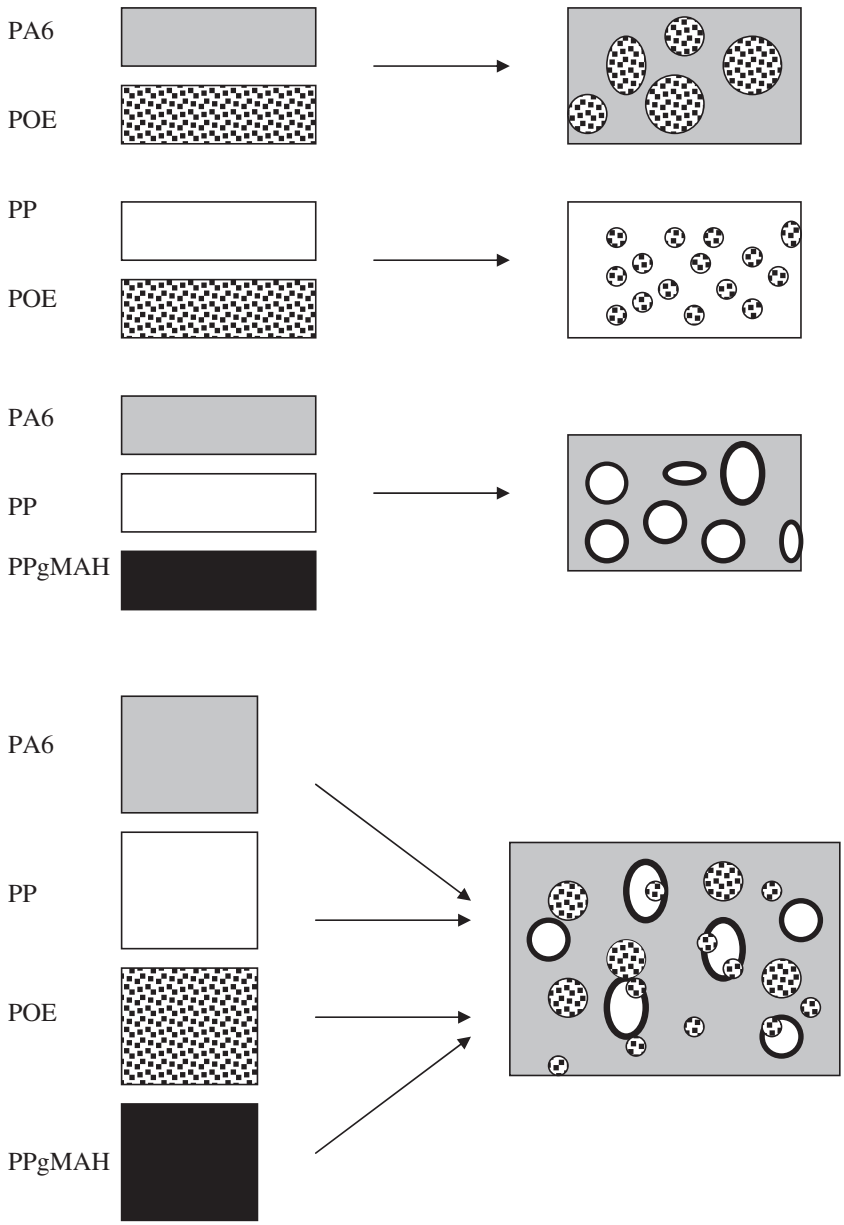

Figure 13. Scheme of morphology of binary and ternary blends of PA6, PP, POE and PPgMAH.

persed in the PA6 phase. While in the ternary blends of PA6/PP/POEgMAH, the rubbers are also located at the PA6/PP interface and in the PA6 phase with smaller particle size. The maleated POE also seems to act as impact modifier for the PA6 phase and as an interfacial compatibilizer for the blends.

CONCLUSION

The addition of elastomer into PA6/PP/organoclay enhances the toughness and ductility but reduces the stiffness and strength of the nanocomposites. Although the modulus and strength of the nanocomposites was not significantly affected by types of elastomer and their functionality, the usage of the maleic anhydride grafted POE and EPR resulted in better toughness properties. This has been attributed to an increase in adhesion between the phases, brought about by the reaction between amino groups of PA6 and anhydride groups of maleated elastomer. The morphology of PA6/PP/organoclay is also affected by the functionality of both POE and EPR. The compatibilization effect of POEgMAH and EPRgMAH is manifested by the morphological transformation as evidenced from SEM analysis.

Acknowledgment. The authors would like to thank Ministry of Science, Technology and Innovation (MOSTI), Malaysia for the IRPA grant (grant no: UTM 74177). Special scholarship (SLAB) granted by Universiti Teknologi Malaysia to one of us (Mr. M. U. Wahit) is gratefully acknowledged.

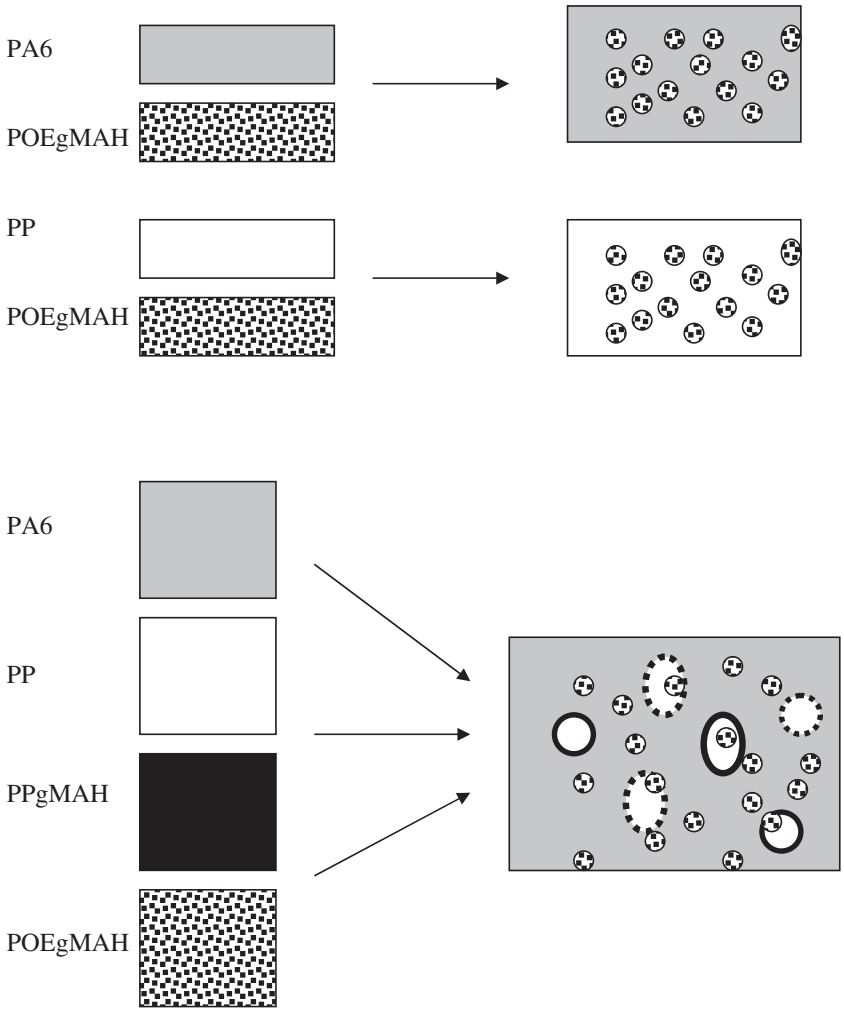

Figure 14. Scheme of morphology of binary and ternary blends of PA6, PP, POEgMAH.

REFERENCES

1. W. S. Chow, Z. A. Mohd Ishak, U. S. Ishiaku, J. Karger-Kocsis, and A. A. Apostolov, *J. Appl. Polym. Sci.*, **91**, 175 (2003).
2. W. S. Chow, Z. A. Mohd Ishak, J. Karger-Kocsis, A. A. Apostolov, and U. S. Ishiaku, *Polymer*, **44**, 7427 (2003).
3. A. G. Montiel, H. Keskkula, and D. R. Paul, *Polymer*, **36**, 4605 (1995).
4. A. G. Montiel, H. Keskkula, and D. R. Paul, *Polymer*, **36**, 4587 (1995).
5. A. G. Montiel, H. Keskkula, and D. R. Paul, *Polymer*, **36**, 4621 (1995).
6. H. Wang, C. Zeng, M. Elkovitch, and L. M. Lee, *Polym. Eng. Sci.*, **41**, 2036 (2001).
7. X. Liu, Q. Wu, L. A. Berglund, J. Fan, and Z. Qi, *Polymer*, **42**, 8235 (2000).
8. S. C. Tjong, S. A. Xu, R. K. Y. Li, and Y. W. Mai, *Mater. Sci. Eng., A*, **347**, 338 (2003).
9. N. Hasegawa, M. Kawasumi, M. Kato, A. Usuki, and A. Okada, *J. Appl. Polym. Sci.*, **67**, 87 (1998).
10. S. L. Bai, G. T. Wang, J. M. Hiver, and C. G'Sell, *Polymer*, **45**, 3063 (2004).
11. D. M. Laura, H. Keskkula, J. W. Barlow, and D. R. Paul, *Polymer*, **44**, 3347 (2003).
12. J. W. Cho and D. R. Paul, *J. Appl. Polym. Sci.*, **80**, 484 (2000).
13. D. M. Laura, H. Keskkula, J. W. Barlow, and D. R. Paul, *Polymer*, **43**, 4673 (2002).
14. M. U. Wahit, A. Hassan, Z. A. Mohd Ishak, and A. Abu Bakar, *Polym. Polym. Compos.*, **13**, 795 (2005).
15. M. U. Wahit, A. Hassan, Z. A. Mohd Ishak, A. R. Rahmat, J. W. Lim, and N. Othman, Proc. Int. Conf. on 'Advances in Polymer Blends, Composites, IPNS and Gel: Macro to Nano Scales (ICBC-2005),' Mahatma Gandhi University, Kerala, India, March 2005, p 38.
16. S. S. Ray and M. Okamoto, *Prog. Polym. Sci.*, **28**, 1539 (2003).
17. M. Alexandre and P. Dubois, *Mater. Sci. Eng.*, **28**, 1 (2000).
18. J. W. Cho and D. R. Paul, *Polymer*, **42**, 1083 (2001).
19. T. X. Liu, Z. H. Liu, K. X. Ma, L. Shen, K. Y. Zeng, and C. B. He, *Compos. Sci. Technol.*, **63**, 331 (2003).
20. N. Hasegawa, H. Okamoto, M. Kawasumi, and A. Usuki, *J. Appl. Polym. Sci.*, **74**, 3359 (1999).
21. J. Duvall, C. Sellitti, C. Myers, A. Hiltner, and E. Baer, *J. Appl. Polym. Sci.*, **52**, 195 (1994).
22. N. Zeng, S. L. Bai, C. G. Sell, J.-M. Hiver, and Y. W. Mai,

Polym. Int., **51**, 1439 (2002).
23. J. C. Stevenson, *J. Vinyl Addit. Technol.*, **1**, 41 (1995).
24. K. T. Gam, M. Miyamoto, R. Nishimura, and H. J. Sue, *Polym. Eng. Sci.*, **43**, 1635 (2003).
25. F. Q. Li, D. G. Kim, D. Z. Wu, K. Lu, and R. G. Jin, *Polym. Eng. Sci.*, **41**, 2155 (2001).
26. Z. Z. Yu, Y. C. Ke, Y. C. Ou, and G. H. Hu, *J. Appl. Polym. Sci.*, **76**, 1285 (1999).
27. K. Premphet-Sirisinha and S. Chalearmthitipa, *Polym. Eng. Sci.*, **43**, 317 (2003).
28. S. Cimmino, F. Coppola, L. D'Orazio, R. Greco, G. Maglio, and M. Malinconoco, *Polymer*, **27**, 1874 (1986).
29. W. G. Perkin, *Polym. Eng. Sci.*, **39**, 2445 (1999).
30. J. Z. Liang and R. K. Y. Li, *J. Appl. Polym. Sci.*, **77**, 409 (2000).
31. S. Thomas and G. Groeninckx, *Polymer*, **40**, 5799 (1999).
32. Y. Long and R. A. Shanks, *J. Appl. Polym. Sci.*, **61**, 1877 (1996).
33. K. Premphet and P. Horanont, *J. Appl. Polym. Sci.*, **76**, 1929 (2000).